

# Coupling Effect of Morphology and Mechanical Properties Contributes to the Tribological Behaviors of Snake Scales

Long Zheng, Yinghui Zhong, Yihang Gao, Jiayi Li, Zhihui Zhang, Zhenning Liu<sup>\*</sup>, Luquan Ren

Key Laboratory of Bionic Engineering (Ministry of Education), College of Biological and Agricultural Engineering, Jilin University, Changchun 130022, China

## Abstract

It is known that the tribological behaviors of snake skins are contributed by the synergistic action of multiple factors, such as surface morphology and mechanical properties, which has inspired fabrication of scale-like surface textures in recent years. However, the coupling effect and mechanism remain to be elucidated. In this work, the morphology and mechanical properties of the scales from different body sections (leading body half, middle trunk and tailing body half) and positions (dorsal, lateral and ventral) of *Boa constrictor* and *Eryx tataricus* were characterized and compared to investigate the corresponding effects on the tribological behaviors and to probe the possible coupling mechanism. The morphological characterizations of scanning electron microscopy and atomic force microscopy revealed significant differences between the two species that the scales from *Boa constrictor* are rougher in general. The mechanical properties measured by nanoindentation corroboratively demonstrated substantial differences in elastic modulus and hardness. Interestingly, the ventral scales with lower surface roughness, together with relatively larger elastic modulus and hardness, manifest higher friction coefficients. A “double-crossed” hypothesis was proposed to explain the observed coupling effect of morphology and mechanical properties on friction, which may afford valuable insights for the design of bionic surface with desirable tribological performance.

**Keywords:** bionics, coupling effect, friction coefficient, morphology, mechanical properties, snake scales

Copyright © 2018, Jilin University.

## 1 Introduction

Evolution and selection in nature has yielded various species with optimized biological features, which have inspired bionic engineering over recent decades<sup>[1–5]</sup>. Snakes are one of nature’s most amazing well-adapted reptilians without extremities, which have evolved over 150 million years and inhabited almost every land on earth<sup>[6,7]</sup>. One interesting trait of snakes is the sliding locomotion, which renders the ventral scales at the belly in direct and continuous contact with the surroundings. Therefore, the snake scales have developed a range of tribological characteristics fitting to respective habitat condition and locomotion, which could afford valuable insights for friction and wear research<sup>[8]</sup>.

Friction remains a big concern in engineering and recently more investigations have been made on the structures and materials of snake scales to achieve better understanding of their frictional behaviors<sup>[8–17]</sup>. In these reported cases, snake scales manifested various desira-

ble performances, such as adhesion reduction<sup>[10]</sup>, wear resistance<sup>[12]</sup> and frictional anisotropy<sup>[15]</sup>. In particular, it has been suggested that distinct skin microstructures account for different frictional properties in discrete body positions<sup>[13]</sup>. It has also been shown that the functional microstructure on scales is an adaptation of snake species to their preferential habitats<sup>[12]</sup>. Moreover, mechanical analysis of snake epidermis has revealed a gradient of hardness and elastic modulus, which corresponds to the respective inhabiting condition, indicating that such a gradient is a potential adaptation to locomotion and wear reduction on substrates<sup>[14,16]</sup>.

The insights gained from the investigations of snake epidermis have inspired various bio-mimicking designs<sup>[18–24]</sup>. For instance, it has been suggested that a surface texture resembling the scale microstructures of the *Python regius* is able to benefit the lubrication of cylinder liners<sup>[18]</sup>. The frictional examination on polymer surface with snake-inspired microstructures has revealed that the special surface morphology of snake

<sup>\*</sup>Corresponding author: Zhenning Liu  
E-mail: [liu\\_zhenning@jlu.edu.cn](mailto:liu_zhenning@jlu.edu.cn)

ventral scales can not only lower friction coefficient, but also generate anisotropic friction, which might be another adaptation to sliding locomotion<sup>[20,21]</sup>.

These works have also indicated that the frictional behaviors of snake skins are contributed by the synergistic actions or coupling effects of multiple factors rather than determined by a single factor<sup>[25,26]</sup>. Yet, the coordinated mechanism of multiple factors remains to be elucidated in order to implement bio-mimicking tribosystems with desirable friction performance.

The objective of the present study is to investigate the effects of morphology and mechanical properties on the frictional behaviors of snake epidermis and to probe the coupling effect between these two factors as a result of possible adaptation. The following three key questions are addressed in this work: (1) What are the major morphological differences between the two surveyed snake species (*Eryx tataricus* and *Boa constrictor*) from different inhabiting conditions, especially with regard to distinct body positions? (2) How do the mechanical properties of scales vary between these two species? (3) How does the coupling of surface roughness and mechanical properties take effect on the frictional behaviors? The shed snake epidermis from *Eryx tataricus* (Squamata) and *Boa constrictor* (Squamata) with different preferential habitats and lifestyles, thus moving on different substrates and under different friction conditions, was compared to answer these questions.

## 2 Materials and methods

### 2.1 Animals

Two snake species, *Boa constrictor* and *Eryx tataricus* of the *Boidae* family, were chosen in this work because they have distinct preferential habitats and lifestyles as well as different body weights.

*Boa constrictor* (Linnaeus, 1758), also called red-tailed boa, is a species of large, heavy-bodied snake in the *Boidae* family. *Boa constrictor* lives in a broad range of environments, from tropical rainforests to arid semidesert country<sup>[27]</sup>. However, it is more often found in rainforests due to the preferred humidity and temperature as well as plenty of potential preys. As semi-arboreal snakes, young *boa constrictors* may climb onto trees and shrubs to prey. However, they become mostly terrestrial as they grow older and heavi-

er<sup>[28]</sup>.

In contrast, *Eryx tataricus*, commonly found in the dessert from the east Caspian Sea to western China and Mongolia, is a relatively smaller and lighter snake in the *Boidae* family, which was first described by Lichtenstein in 1823<sup>[29]</sup>. It normally burrows under sands or rocks *via* the locomotion of lateral undulation at a relative slow speed. The inhabiting conditions of *Eryx tataricus* are arid and warm.

The animals were reared in 80 cm×60 cm×60 cm (length×width×height) wood cabinets under same controlled temperature (around 26 °C) and humidity (around 38% RH) at Jilin University, China. The bottom of the cabinet for *Eryx tataricus* was covered by a sand layer of roughly 10 cm, whereas no sand was added to the cabinet for *Boa constrictor*. Two adult mice were fed twice a week. All samples examined in this study were shed skins derived from a 5 year-old male *Eryx tataricus* (body mass of 0.25 kg and length of 115 cm, top panel in Fig. 1) and a 3 year-old male *Boa constrictor* (body mass of 0.7 kg and length of 163 cm, bottom panel in Fig. 1).

To characterize the morphological features of the shed skins from different body positions (dorsal, lateral and ventral), the snakes are divided into three sections (Fig. 1), as previously described<sup>[30]</sup>. The first one is denoted as Leading Body Half (LBH) near the head. The stockiest portion of the body is regarded as Middle Trunk Section (MTS), which follows LBH as the second section. The remaining portion is named as Tailing Body Half (TBH), which accounts for approximately the same ratio as LBH but near the tail.

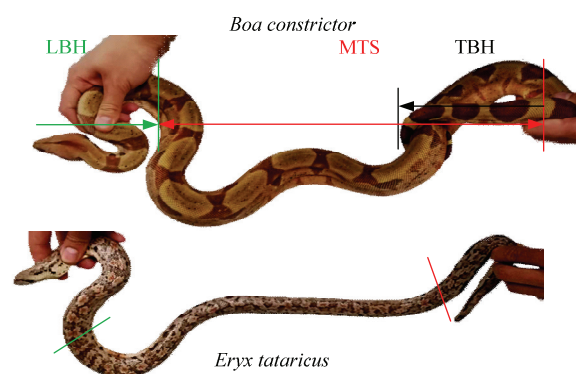


**Fig. 1** The photographs of *Boa Constrictor* and *Eryx tataricus*. LBH: Leading Body Half (about 20% of the total length); MTS: Middle Trunk Section (about 65% of the total length); TBH: Tailing Body Half (about 15% of the total length).

## 2.2 Sample collection and treatments

The epidermis of adult individuals was collected directly after shedding from the cabinets and washed repeatedly to remove excreta, followed by soaking in distilled water for 4 h at room temperature to unfold the wrinkles. Subsequently the shed skins were wiped with paper towels. Then the shed skins were dried by a hair dryer and wrapped in baking paper, which were then stored in sealed plastic bags at room temperature until use.

## 2.3 Scanning Electron Microscopy (SEM)

The samples of dorsal, lateral and ventral scales from three sections of the two species were cut into 5 mm × 5 mm pieces and mounted on microscope slides with cyanoacrylate adhesive (Ruichang Gold 3-Second Ltd. Co., China). The mounted samples were sputtering-coated with gold-palladium (~10 nm in thickness) and then observed by a SEM (Zeiss EVO 18, England, Cambridge) at an accelerating voltage of 20 kV.

## 2.4 Atomic Force Microscopy (AFM)

The surface profiles of the samples were obtained by AFM (Bruker Dimension ICON, America) under the ScanAsyst-air contact mode. Scans were carried out at room temperature with a scan rate of 1 Hz and a resolution of 256 × 256 pixels using a ScanAsyst-air cantilever. The width, depth and height between two micro-units were estimated from AFM images processed by NanoScope (Bruker GmbH, German, version 1.40). The average roughness of samples was calculated with the same software.

## 2.5 Nanoindentation

The nanoindentation measurements were performed on an Agilent Nano Indenter G200 equipped with a Berkovich tip at a drift rate of 0.1 nm·s<sup>-1</sup>. All measurements were conducted with Poisson ratio of 0.3 and peak hold time of 50 s at room temperature. Herein, two different modes were used. First, under the basic mode, the elastic moduli and hardnesses of scales (5 mm × 5 mm) were examined by following the line of circles from the anterior edge to the posterior edge with a spacing of 300 μm, as depicted in Fig. 2a. At least 5 independent indentations with a spacing of 50 μm were

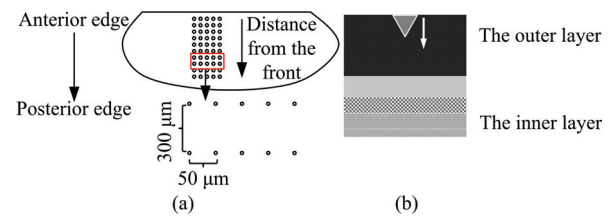


**Fig. 2** Schematic illustration of nanoindentation measurements. (a) The indented points on a single scale with circles representing test points; (b) the illustration of a probe penetrating the scale vertically to measure elastic modulus and hardness with increasing penetration depth. The inverted triangle represents the probe.

carried out at each distance denoted from the front (Fig. 2a). The elastic moduli and hardnesses of the samples were then calculated from the force and displacement curves. Second, the Continuous Stiffness Measurement (CSM) mode was adopted on the ventral scales of *Boa constrictor* with a penetration depth up to 12000 nm (Fig. 2b) to acquire the profiles of elastic modulus and hardness with respect to penetration depth.

## 2.6 Friction measurements

Dynamic frictional measurements were conducted on a nanotribo-meter (NTR<sup>2</sup>, Anton Paar Company, Switzerland) under the linear reciprocating sliding mode with a maximum linear speed of 63 μm·s<sup>-1</sup> and a stroke of 1 mm. The applied normal force was 0.6 mN. The samples (dorsal, lateral and ventral scales) were tested against a smooth, spherical silicon carbide probe (diameter ≈ 2 mm) under a dry-sliding contact condition at room temperature (RH ≈ 40%). All samples were mounted on microscope slides using cyanoacrylate adhesive. The samples were tested in the forward, backward and transverse directions. For each kind of scale, six parallel measurements were carried out. The friction coefficients were recorded by the machine and statistically analyzed with Origin (version 8.5) and SPSS (version 22.0) (Students' *t*-test).

## 3 Results

### 3.1 Morphology on scale surface

Previous work has demonstrated that scale microstructures play important roles in the tribological properties of snake skins<sup>[31–33]</sup>. Hence, we first set out to examine the microstructures of shed scales from *Boa*

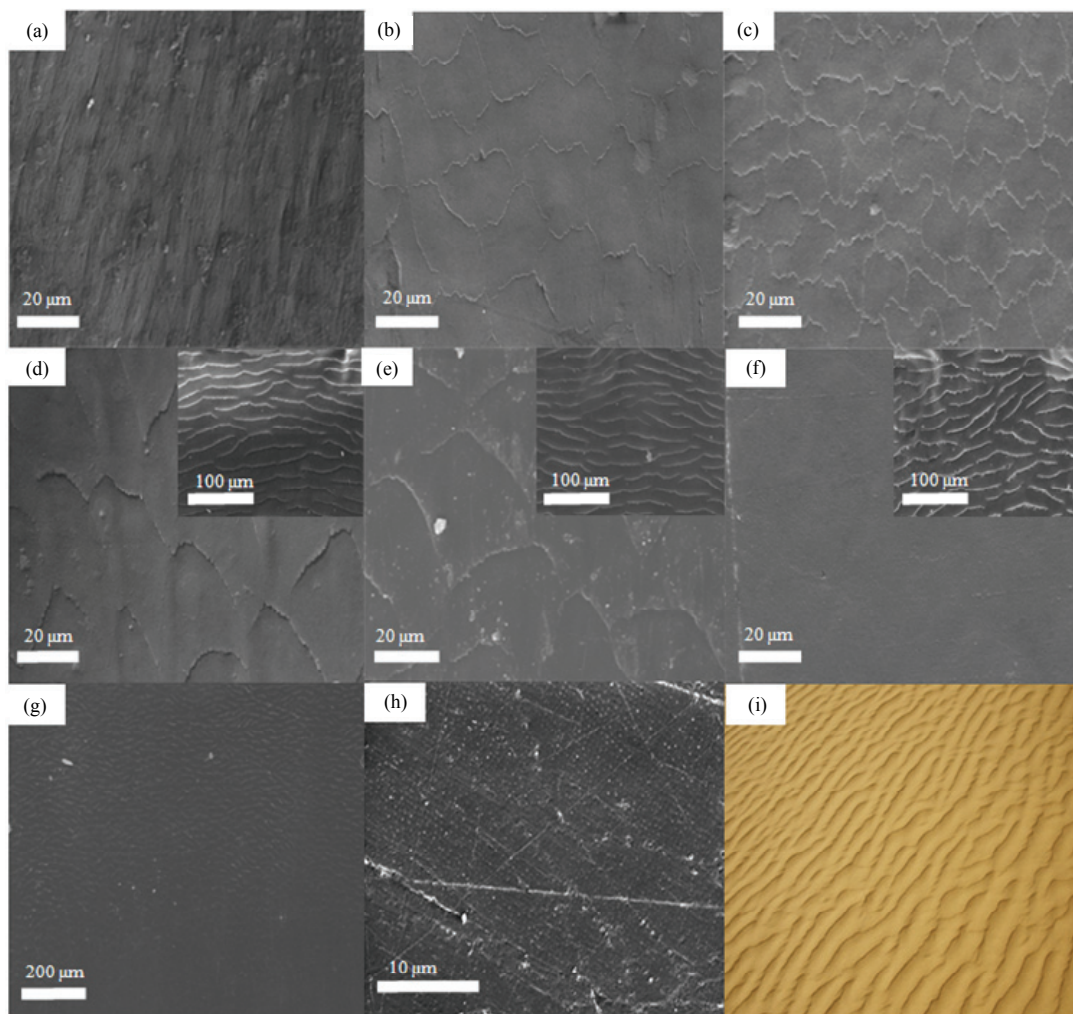


**Fig. 3** SEM images of shed scales (a–h) from two species and a photograph of aeolian sand ripple (i). (a), (b) and (c) show dorsal, lateral and ventral scales from the MTS of *Boa constrictor*. (d), (e) and (f) exhibit dorsal, lateral and ventral scales from the MTS of *Eryx tataricus*. The insets in (d), (e) and (f) are the microstructures on the front edges of respective scales of *Eryx tataricus*. (g) is an image of the transition from the front edge to the middle portion of the ventral scale of *Eryx tataricus*. Anterior is oriented at the top in image (a–g). (h) shows scratches and wear patterns on the ventral scale surface of *Eryx tataricus*. (i) is a photograph of aeolian sand ripple as a comparison (a courtesy from Sina website).

*constrictor* and *Eryx tataricus* by SEM (Fig. 3). Generally speaking, the microstructures on lateral scales from MTS of *Boa constrictor* (Fig. 3b) and *Eryx tataricus* (Fig. 3e) exhibit similar patterns of roughly longitudinal-aligned flakes with overlapping-caused ridges, whereas the dorsal (Figs. 3a and 3d) and ventral (Figs. 3c and 3f) scales reveal different micro-morphologies for two species. The surface patterns on the ventral scale of *Boa constrictor* (Fig. 3c) and the dorsal scale of *Eryx tataricus* (Fig. 3d) resemble the common feature observed for the lateral scales. In contrast, well-aligned ridges paralleled to the longitudinal body axis are found

on the dorsal scales from the MTS of *Boa constrictor* (Fig. 3a). Moreover, the SEM image of the ventral scales from the MTS of *Eryx tataricus* display a relatively smooth morphology with no practically discernible micro-ornaments at the same magnification (Fig. 3f), which is in sharp contrast to those of the dorsal and lateral scales. Random scratches and wear patterns have been frequently found on these ventral scales (Fig. 3h). It is noteworthy that the front edges of the scales of *Eryx tataricus* are mounted by tiny wrinkles (insets in Figs. 3d–3f), which differ from the major portions of scales (Figs. 3d–3f) and look like aeolian sand ripples

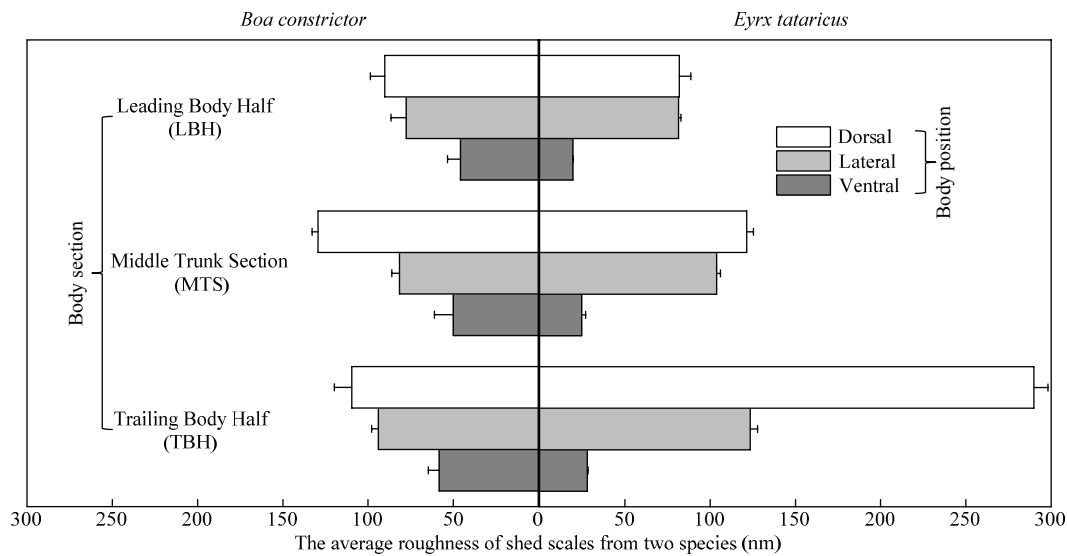


**Fig. 4** The average roughness ( $R_a$ ) of scales in different body positions and sections of *Boa constrictor* and *Eryx tataricus*. The error bars denote standard deviations.

(Fig. 3i). The transition from ripple-like wrinkles to smooth surface is also verified, as shown in Fig. 3g.

Surface roughness is one key parameter for morphological characterization that plays an important role in surface friction<sup>[23,34]</sup>. Hence, the average surface roughness ( $R_a$ ) of the scales from LBH, MTS and TBH of *Boa constrictor* and *Eryx tataricus* was measured by AFM (Fig. 4). Overall, the ventral scales of the two species demonstrate obviously lower  $R_a$  than the other body positions, albeit with microstructures on the scale surface. With regard to different body sections of the two species, the  $R_a$  of scales from LBH, MTS and TBH exhibit a consistent trend of dorsal > lateral > ventral with one exception at the LBH of *Eryx tataricus*, where the dorsal and lateral scales display comparable roughness. Moreover, the comparison between *Boa constrictor* and *Eryx tataricus* reveals a most prominent difference for dorsal scales at TBH.

In order to gain a better understanding of the above trends, the parameters of unit microstructures, including the width, depth and height of micro-units, were extracted from AFM profiles and compared (Fig. 5 and Table 1). It is found that the widths, depths and heights of lateral scale units in different body sections of *Boa constrictor* are significantly larger than those of respective ventral scale units. In contrast, the widths and depths of dorsal scale units in different body sections of *Eryx*

*tataricus* are close to those of respective lateral scale units, with one exception that the depth of dorsal scale units at TBH is more than three times of the depth of lateral scale units. In addition, the heights of dorsal scale units in different body sections of *Eryx tataricus* are also larger than those of lateral scale units. In particular, for TBH the height of dorsal scale units is approximately 6.5 times of the height of lateral scale unit. These parameters (Table 1) have corroborated the measured roughness (Fig. 4) in following aspects: first, for *Boa constrictor*, lateral scales are rougher than ventral scales regardless of body sections; second, for *Eryx tataricus*, the roughness of dorsal scales and lateral scales are comparable at LBH and MTS; third, the dorsal scales at TBH of *Eryx tataricus* show more dramatic micro-patterning and thus higher roughness. It should be noted that it is difficult to extract unit parameters for the dorsal scales of *Boa constrictor* and the ventral scales of *Eryx tataricus*.

### 3.2 Mechanical properties of scales

It has been reported that snake skins are equipped with anti-wear functions owing to their mechanical properties<sup>[14]</sup>. To this end, nanoindentation was utilized to characterize the mechanical properties (*i.e.* elastic modulus and hardness) of scales in different body positions and sections from *Eryx tataricus* and *Boa*

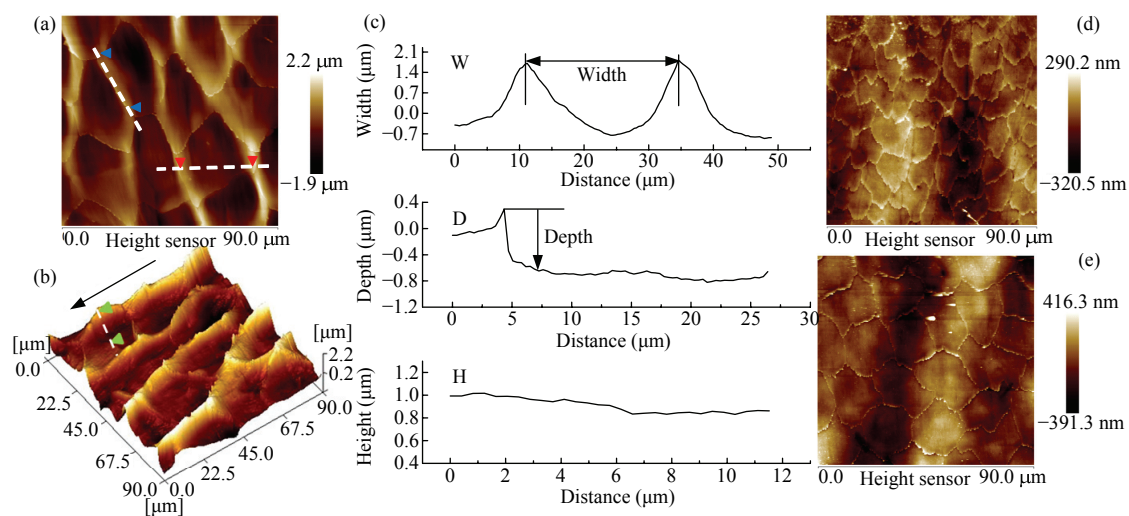


**Fig. 5** Representative AFM images (a, b, d and e) and parameter extractions from AFM profiling. (a) is an AFM image of microstructures on the dorsal scale of TBH from *Eryx tataricus* with indicated width profiling (between two red arrowheads) and height profiling (between two blue arrowheads). (b) is the 3D image of (a) with indicated depth profiling (between two green arrowheads). The black arrow on the side points to the posterior in (b). (c) shows the width (top), depth (middle) and height (bottom) profiles along the corresponding lines in (a) and (b). The width, depth and height extracted from (c) are 23.761  $\mu\text{m}$ , 0.989  $\mu\text{m}$  and 0.916  $\mu\text{m}$ , respectively. (d) and (e) are AFM images of microstructures on the ventral and lateral scales of MTS from *Boa constrictor*. W: the width between the two units of microstructures. D: the height difference between the ridge and the valley. H: the height measured along the ridge.

**Table 1** Parameters for unit microstructures on scales from *Boa constrictor* and *Eryx tataricus*

Scales	Width ( $\mu\text{m}$ )	Depth ( $\mu\text{m}$ )	Height ( $\mu\text{m}$ )
<b><i>Boa constrictor</i></b>			
Ventral (LBH)	13.362 $\pm$ 1.647	0.128 $\pm$ 0.010	0.036 $\pm$ 0.008
Ventral (MTS)	13.221 $\pm$ 0.640	0.139 $\pm$ 0.011	0.060 $\pm$ 0.009
Ventral (TBH)	18.557 $\pm$ 0.786	0.138 $\pm$ 0.015	0.042 $\pm$ 0.005
Lateral (LBH)	20.727 $\pm$ 0.967	0.173 $\pm$ 0.015	0.073 $\pm$ 0.012
Lateral (MTS)	20.509 $\pm$ 0.858	0.258 $\pm$ 0.017	0.082 $\pm$ 0.010
Lateral (TBH)	25.457 $\pm$ 1.097	0.203 $\pm$ 0.012	0.055 $\pm$ 0.011
<b><i>Eryx tataricus</i></b>			
Dorsal (LBH)	25.536 $\pm$ 1.850	0.321 $\pm$ 0.017	0.144 $\pm$ 0.011
Dorsal (MTS)	27.751 $\pm$ 1.018	0.494 $\pm$ 0.049	0.134 $\pm$ 0.015
Dorsal (TBH)	23.229 $\pm$ 1.067	0.992 $\pm$ 0.114	1.036 $\pm$ 0.125
Lateral (LBH)	28.610 $\pm$ 1.945	0.344 $\pm$ 0.037	0.104 $\pm$ 0.016
Lateral (MTS)	28.022 $\pm$ 0.961	0.451 $\pm$ 0.036	0.127 $\pm$ 0.014
Lateral (TBH)	26.908 $\pm$ 1.124	0.281 $\pm$ 0.055	0.159 $\pm$ 0.017

*constrictor* (Figs. 6–8). Fig. 6a exhibits elastic moduli and hardnesses of a single scale with different penetration depths in the vertical direction. Consistent with previous findings<sup>[14]</sup>, the measured elastic moduli and hardnesses become relatively stable beyond the penetration depth of 200 nm. Then the elastic modulus displays a slight rise as the penetration increases, whereas the hardness slowly declines. Such a depth-correlated gradient has also been reported by other groups<sup>[16]</sup>. It is

noted that the elastic modulus and hardness are almost constant at depth from 200 nm to 2000 nm (inset in Fig. 6a). Therefore, the elastic moduli and hardnesses at the depth of 1000 nm were measured from anterior to posterior on a single scale, as depicted in Fig. 2, to examine the horizontal changes of mechanical properties on scale surfaces. Figs. 6b and 6c show the elastic moduli and hardnesses of ventral scales from different body sections of *Eryx tataricus*, respectively.

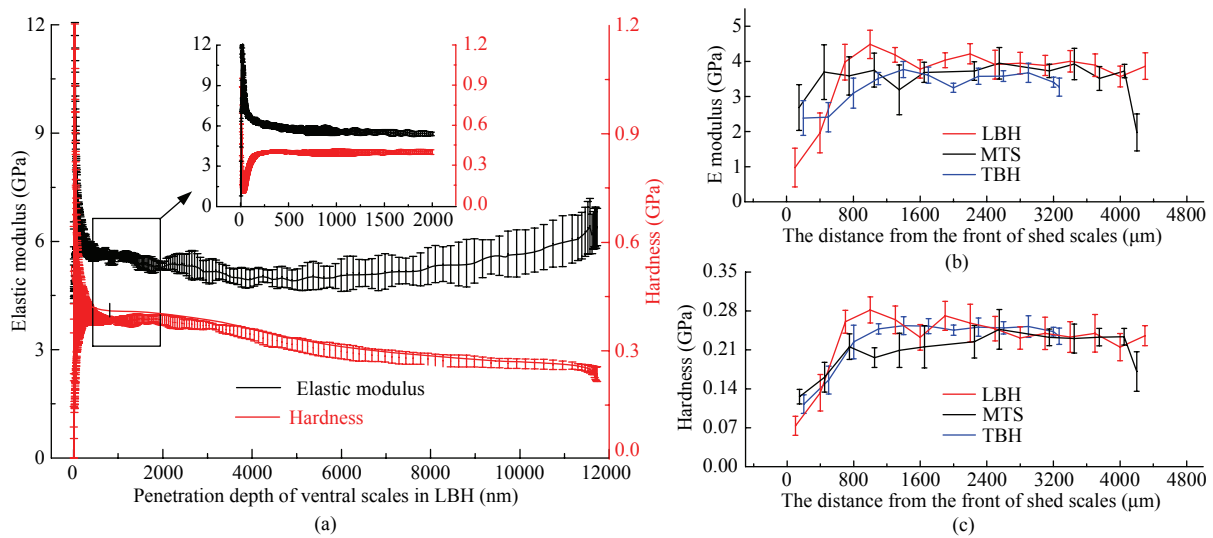


**Fig. 6** Elastic moduli and hardnesses of ventral scales in different sections of *Boa constrictor* and *Eryx tataricus*. (a) exhibits elastic moduli (black) and hardnesses (red) of ventral scales from *Boa constrictor* at different penetration depths. The inset shows elastic moduli and hardnesses of ventral scales at the depth of 200 nm – 2000 nm. (b) and (c) show elastic moduli and hardnesses from anterior to posterior on ventral scales in different sections of *Eryx tataricus*, respectively. The error bars denote standard deviations.

Interestingly, both elastic modulus and hardness are low near the front edge and gradually elevate to a steady level, indicating a horizontal gradient of mechanical properties also exists on the snake scale and the snake body as a whole can be regarded as an integration of alternating hard-soft materials.

In order to compare the mechanical properties of scales across the whole body for the two species, nanoindentation (at penetration depth of 1000 nm) was carried out at the middle of scales from different body positions and sections, where the elastic modulus and hardness maintained a relatively stable level. Overall, the hardnesses of the two species are comparable, with those of *Boa constrictor* being a slightly higher (lines in Fig. 7). Yet, the scales of *Boa constrictor* exhibit generally larger elastic moduli than the counterpart of *Eryx tataricus* (histograms in Fig. 7). A common order of lateral < dorsal < ventral is also found for the elastic moduli and hardnesses of scales in different body sections of the two snakes, except that the hardness of dorsal scales at TBH of *Boa constrictor* is a bit smaller than that of respective lateral scales (Fig. 7).

Pairwise statistical analyses (Students' *t*-test) were performed on the elastic moduli and hardnesses of scales in different body positions (dorsal, lateral and ventral)

and sections (LBH, MTS and TBH) for individual species (Fig. 8). The white boxes (diagonal from top left to bottom right in Fig. 8) show the significant differences among dorsal, lateral and ventral scales in the same body sections for *Boa constrictor* (Figs. 8a and 8b) and *Eryx tataricus* (Figs. 8c and 8d) in terms of elastic modulus (Figs. 8a and 8c) and hardness (Figs. 8b and 8d). It is found that both species exhibit a comparable pattern of elastic modulus differences with substantially lower elastic moduli for the lateral scales at distinct body sections (white boxes in Figs. 8a and 8c), whereas the differences for scale hardnesses from *Eryx tataricus* are more significant than those from *Boa constrictor*, especially at LBH (top left white boxes in Figs. 8b and 8d). The colored boxes (filled with orange, blue and green) display the significant differences among LBH, MTS and TBH at the same body positions for the two species. It is noted that for elastic modulus and hardness, body sections play a more important role for scales from *Eryx tataricus* than those from *Boa constrictor*, particularly for the comparisons of MTS vs. LBH and MTS vs. TBH (orange and blue boxes in Fig. 8). In summary, the mechanical properties of scales show dramatic variations for *Eryx tataricus* with regard to both body positions and sections, whereas body positions are more dominant in scale mechanical performance than body sections for

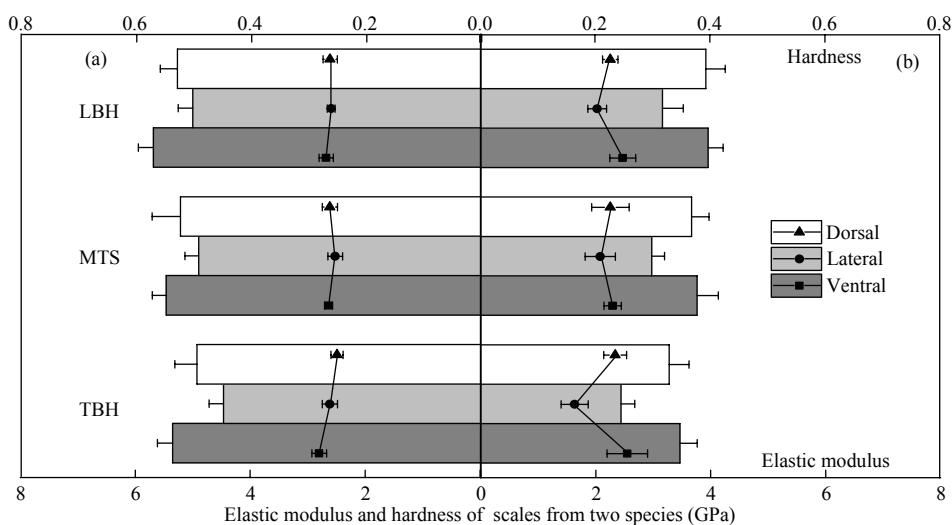


**Fig. 7** Elastic moduli (histograms) and hardnesses (lines) of scales at different body positions and sections of *Boa constrictor* (a) and *Eryx tataricus* (b). The error bars denote standard deviations.

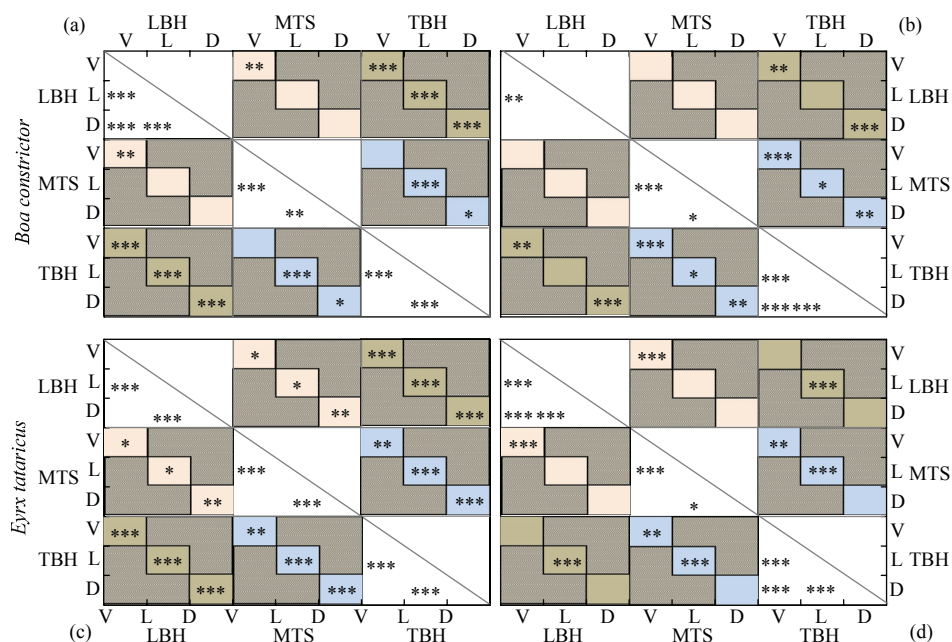


**Fig. 8** The significant differences of mechanical properties for scales from different body positions and sections of *Boa constrictor* (a and b) and *Eryx tataricus* (c and d). (a) and (c) show the significant differences of elastic modulus for *Boa constrictor* and *Eryx tataricus*, respectively. (b) and (d) exhibit the significant differences of hardness for *Boa constrictor* and *Eryx tataricus*, respectively. Significance of Students' *t*-test: \* for  $p < 0.05$ ; \*\* for  $p < 0.01$ ; \*\*\* for  $p < 0.001$ . D: dorsal scales; L: lateral scales; V: ventral scales. Diagonal white boxes are the significant differences for scales at the same body section but different positions. Orange, blue and green boxes are the significant differences for scales at the same body position but different sections. The grey boxes are not applicable.

*Boa constrictor*.

### 3.3 Tribological behaviors of scales

Anisotropic frictional properties have been demonstrated for scales of *Lampropeltis getula californiae*<sup>[35]</sup>. Herein, the friction coefficients of the scales

from MTS of two species were measured in different rubbing directions by a nanotribometer to investigate the anisotropic frictional properties of scales in different body positions (Fig. 9). The friction coefficients were acquired in three directions: forward (F), backward (B) and transverse (T). Overall, the friction coefficients of



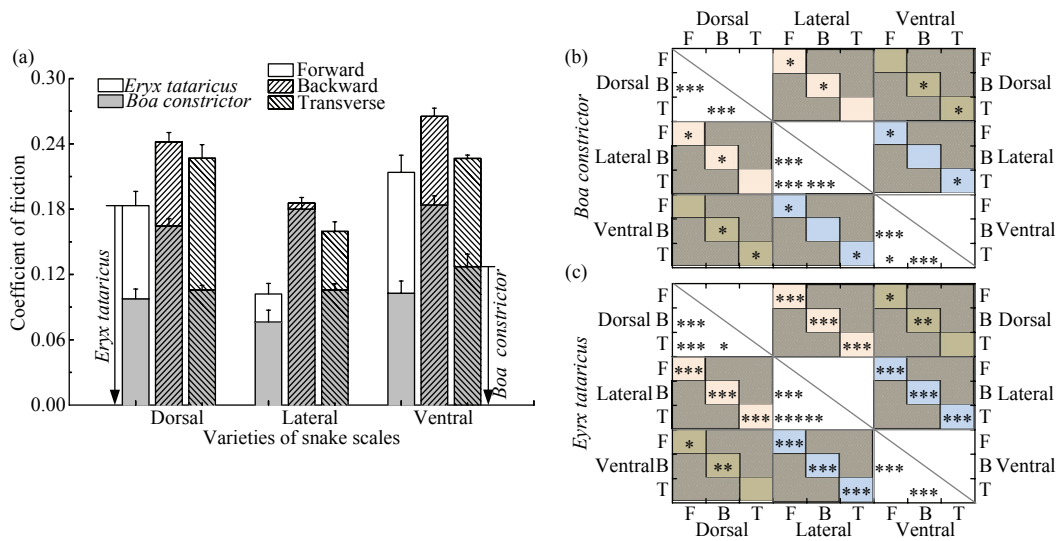


**Fig. 9** Anisotropic friction coefficients for scales in MTS of *Boa constrictor* and *Eryx tataricus*. (a) shows frictional coefficients of different rubbing directions for dorsal, lateral and ventral scales in MTS of *Boa constrictor* and *Eryx tataricus*. The error bars denote standard deviations. (b) and (c) are the significant differences of frictional coefficients in panel (a). Significance of Students' *t*-test: \* for  $p < 0.05$ ; \*\* for  $p < 0.01$ ; \*\*\* for  $p < 0.001$ . F: forward; B: backward; T: Transverse. Diagonal white boxes are the significant differences for friction coefficients of the same body position but different rubbing directions. Orange, blue and green boxes are the significant differences for friction coefficients of the same rubbing direction but different body positions. The grey boxes are not applicable.

scales from *Eryx tataricus* are larger than those of the counterparts from *Boa constrictor* (buildup boxes in Fig. 9a), particularly at dorsal and ventral positions. Moreover, the ventral scales show higher friction than other positions in general for each species. It is also apparent that for both species, the friction coefficients of the backward direction are higher than those of the other directions, indicating evident friction anisotropy.

Pairwise statistical analyses (Students' *t*-test) were also carried out on the friction coefficients in three directions for each species (Figs. 9b and 9c). The white boxes (diagonal from top left to bottom right in Figs. 9b and 9c) show the significant differences of friction coefficients among forward (F), backward (B) and transverse (T) directions at the same body positions for *Boa constrictor* (Fig. 9b) and *Eryx tataricus* (Fig. 9c). The colored boxes (filled with orange, blue and green) display the significant differences of friction coefficients with the same directions among dorsal, lateral and ventral scales for the two species. Interestingly, both species show a comparable pattern of friction coefficient differences at the same body positions (white boxes in Figs. 9b and 9c) indicating an evident anisotropic frictional performance, whereas the differences of the same rubbing direction at different body positions (dorsal, lateral

and ventral scales) from *Eryx tataricus* are more significant than those from *Boa constrictor*, especially for dorsal vs. lateral and ventral vs. lateral (orange and blue boxes in Figs. 9b and 9c). In summary, the scales of the two species exhibit significant anisotropic frictional properties, while the differential friction behavior due to body positions is more prominent for *Eryx tataricus* than that for *Boa constrictor*.

#### 4 Discussion

This work investigated the morphology, mechanical properties and frictional behaviors of the scales from *Boa constrictor* and *Eryx tataricus*. Our morphological characterizations and nanoindentation measurements have corroboratively revealed substantial differences between the two species in terms of morphology, surface roughness and mechanical properties. Simultaneously, friction coefficients of scales in different body positions from the two snakes also exhibit significant anisotropy. Interestingly, the ventral scales show higher friction coefficients but lower surface roughness, together with relatively larger elastic modulus and hardness. Based on these results, we proposed an assumption that the frictional performance of the scales, particularly some unexpected results, is owing to the coupling effect of the

morphology and mechanical properties. This view is also supported by another recent work, which hypothesized that the abrasive resistance of snake scales is not only due to a gradient in material properties of the scales, but also influenced by the morphology of scales<sup>[7]</sup>.









Both SEM and AFM images show that the morphologies on the scale surface are visibly different between the two species (Fig. 3 and Fig 5). The morphological divergence is likely a consequence of both respective inhabiting environments and different locomotion. *Boa constrictor* lives in a broad range of environments, which are less demanding in general compared to those of *Eryx tataricus*<sup>[27]</sup>. Thus, although the MTS of *Boa constrictor* takes more responsibility in its locomotion, the microstructure of ridges on the belly ventral scales is still evident. In contrast, the *Eryx tataricus* mainly resides in deserts and its ventral scales show an almost smooth surface of low roughness without clearly discernible micro-ornaments, probably caused by constant wearing on sand. Moreover, the whole body of *Eryx tataricus* is used in movement, especially in sand burrowing, which suggests that the dorsal and lateral scales also function in propulsion. Hence, the morphology observed on the dorsal and lateral scales from *Eryx tataricus* is similar to those seen on the ventral scales from MTS of *Boa constrictor*, which can be rationalized by the need to generate propulsion force.

More interestingly, the front edges of the scales of *Eryx tataricus* are mounted by tiny wrinkles resembling aeolian sand ripples. It is known that these sand ripples are resulted by repeated erosions of two-phase flow, or airflow, over a long time<sup>[36,37]</sup>. Such a resemblance may not simply be a coincidence. Instead, it suggests that the morphology on the scales of *Eryx tataricus* could also be shaped by the factors that drive the formation of sand ripples. Furthermore, the patterns on the middle portions of dorsal and lateral scales from *Eryx tataricus* can be considered as the derivatives of the front-edge wrinkles, whereas the middle section of ventral scales only retain indiscernible microstructures due to more wearing. Together, the microstructures on the scale surface of *Eryx tataricus* may be an optimal formation adapting to the desert and sand-burrowing lifestyle. In contrast, there is no such a strong relationship between the morphologies of the scales from *Boa constrictor*, assumingly due to its

more complex surroundings and sophisticated lifestyle.

In terms of mechanical properties, both vertical and horizontal gradients are found on the scales of the two snakes (Fig. 6). The layout of repeating gradients on the whole snake body renders an integrated pattern of alternating hard-soft materials, which may afford an anti-wear function in its locomotion. The soft portions in the scales may not only extend and contract with muscle action during locomotion, but also dissipate the stress on the hard portions to reduce fatigue. Instead, the hard portions are equipped with higher elastic modulus to resist deformation as well as abrasive wear. Comparatively, the scales of *Boa constrictor* have larger elastic moduli and hardnesses than those of *Eryx tataricus*, which is likely to overcome greater own body weight. Furthermore, the ventral scales in the same body sections of the two species are of the largest elastic moduli and hardnesses (Fig. 7), which may contribute to forward propulsion by increasing the friction during the undulation locomotion, as discussed below.

To our surprise, the investigation on the tribological behaviors of the scales from the two species revealed higher friction coefficients for the ventral scales (Fig. 9a), which are of least surface roughness (Fig. 4) but relatively larger elastic modulus and hardness (Fig. 7). Intuitively, it is assumed that lower surface roughness with higher mechanical strength would result in less friction according to daily observations. However, such a notion gained on macro-scale structures may not be applicable to the situation of micro-morphology, where the physics could deviate from the classics due to the reason remaining unclear to date. In our case of snake scales, the friction is influenced by both the roughness of surface morphology and the mechanical properties. In order to qualitatively illustrate the coupling effect of such two dimensions on friction, a 2×2 graph was plotted assigning “+” and “-” signs to these factors based on the common beliefs of their impact on friction. For roughness, high roughness and low roughness are given “+” and “-” signs, respectively. For mechanical properties, high elastic modulus and hardness is considered as a benefit for low friction and thus given a “-” sign, whereas the opposite “+” sign represents low elastic modulus and hardness. In Fig. 10, double “+” or “-” would result in high friction due to a coupling effect of

		Roughness	
		Low 	High 
E modulus/Hardness	High 	 High friction by “double - crossed” coupling	 Low friction
	Low 	 Low friction	 High friction by “normal” coupling

**Fig. 10** The illustration for the “normal” and “double-crossed” coupling mechanism of morphology and mechanical properties on frictional behaviors.

two factors. The “normal” coupling of high roughness (+) and low elastic modulus and hardness (+) is understandable (bottom right box), as seen with Velcro. On the contrary, the synergistic increase of friction due to the “double-crossed” coupling of low roughness (–) and high elastic modulus and hardness (–) is counterintuitive (upper left box), with the mechanism being elusive. One possible explanation is that the undeformable surface can retain more stress on the friction interface, which affords more driving force for molecular interaction, and meanwhile, the smooth morphology is able to maximize the real contact area of the friction to engage more molecules for interaction. Hence, in comparison with the lateral scales, the ventral scales of the two species, albeit with lower surface roughness and larger elastic modulus and hardness, have demonstrated higher friction coefficients. Such a coupling effect on ventral scales may also be an adaptation to sliding locomotion, which not only smoothens the ventral surface, but also demands more load-bearing capability at the belly.

Moreover, such a coupling effect of morphology and mechanical properties is not unique to snakes and is not limited to the scenarios of double “+” or “–” signs. Indeed, our previous work has demonstrated that non-smooth biological surfaces with high roughness (“+” sign in Fig. 10) and large elastic modulus or hardness (“–” sign in Fig. 10), as observed on pangolins or beetles, can result in low friction and high wear resistance during movements<sup>[25,38–41]</sup>. Such a coupling effect has been verified on metal surfaces with moderate

roughness, which show enhanced tribological performance than the smooth counterpart<sup>[42,43]</sup>. On the one hand, these work indicates that carefully designed roughness (“+” sign in Fig. 10) on hard surface (“–” sign in Fig. 10) can reduce friction and wear (upper right box). On the other hand, it can also be inferred from the smooth control specimens in these work that low roughness (“–” sign in Fig. 10) on hard surface (“–” sign in Fig. 10) may result in a “double-crossed” coupling effect (upper left box), as what we have observed on these two snake species herein.

In addition, our tribological characterization has also revealed obvious anisotropic friction for the two snakes (Fig. 9a), corroborated by previous studies<sup>[44]</sup>. Based on the previous work, it is assumed that the ridge-like or transverse microstructures provide propulsion force for snakes, almost perpendicular to the direction of locomotion. Moreover, the patterns on the scale surfaces incur an interlocking effect with the irregularities and asperities of the ground, which leads to high friction to prevent slithering in the backward direction<sup>[45]</sup>. Thus, the anisotropic frictional behavior of snake scales is a consequence of evolution adapting to locomotion and lifestyles.

## 5 Conclusion

In this work, the morphology and mechanical properties of the scales from different body sections and positions of *Boa constrictor* and *Eryx tataricus* were characterized and compared to investigate the corresponding effects on the tribological behaviors and to probe the possible coupling mechanism. The morphological characterizations of SEM and AFM revealed significant differences between the two species with the roughness of scales from *Boa constrictor* being larger in general. The mechanical properties measured by nanoindentation corroboratively demonstrated substantial differences in terms of elastic modulus and hardness. Meanwhile, tribological characterizations of scales in different body positions from the two species also exhibited evident anisotropy. Interestingly, the ventral scales manifested higher friction coefficients but lower surface roughness, together with relatively larger elastic modulus and hardness. A “double-crossed” hypothesis was proposed to explain the observed coupling effect of

the morphology and mechanical properties on friction, which may afford valuable insights for the design of materials with desirable tribological performance.

## Acknowledgment

This work was supported by National Natural Science Foundation of China (51375204 and U1601203), Jilin Provincial Science & Technology Department (20140101056JC), and Province Joint Fund (SXGJSF2017-2-4 and SXGJQY2017-1) and JLUSTIRT Program of Jilin University.

The authors thank Dr. Zhonghao Jiang from College of Materials Science and Engineering, Jilin University, for the help on nanoindentation tests and Dr. Zhanjiang Yu from Changchun University of Science and Technology for the help on tribological measurements.

## References

- [1] Ball P. Engineering shark skin and other solutions. *Nature*, 1999, **400**, 507–509.
- [2] Meyers M A, Chen P-Y, Lin A Y-M, Seki Y. Biological materials: Structure and mechanical properties. *Progress in Materials Science*, 2008, **53**, 1–206.
- [3] Wong T-S, Kang S H, Tang S K Y, Smythe E J, Hatton B D, Grinthal A, Aizenberg J. Bioinspired self-repairing slippery surfaces with pressure-stable omniphobicity. *Nature*, 2011, **477**, 443–447.
- [4] Huang H, Zhang Y, Ren L Q. Particle Erosion resistance of bionic samples inspired from skin structure of desert lizard, *Laudakin stoliczkanus*. *Journal of Bionic Engineering*, 2012, **9**, 465–469.
- [5] Comanns P, Winands K, Pothen M, Bott R A, Wagner H, Baumgartner W. The Texas horned lizard as model for robust capillary structures for passive directional transport of cooling lubricants. *SPIE Smart Structures and Materials+ Nondestructive Evaluation and Health Monitoring*, 2016, 979711, <https://doi.org/10.1117/12.2218873>.
- [6] Evans S E. At the feet of the dinosaurs: The early history and radiation of lizards. *Biological Reviews*, 2003, **78**, 513–551.
- [7] Klein M-C G, Gorb S N. Ultrastructure and wear patterns of the ventral epidermis of four snake species (Squamata, Serpentes). *Zoology*, 2014, **117**, 295–314.
- [8] Abdel-Aal H A, Vargiolu R, Zahouani H, El Mansori M. Preliminary investigation of the frictional response of reptilian shed skin. *Wear*, 2012, **290-291**, 51–60.
- [9] Hazel J, Stone M, Grace M S, Tsukruk V V. Nanoscale design of snake skin for reptation locomotions via friction anisotropy. *Journal of Biomechanics*, 1999, **32**, 477–484.
- [10] Arzt E, Gorb S, Spolenak R. From micro to nano contacts in biological attachment devices. *Proceedings of the National Academy of Sciences*, 2003, **100**, 10603–10606.
- [11] Rechenberg I. Tribological characteristics of sandfish. *Nature as Engineer and Teacher: Learning for Technology from Biological Systems*, 2003, 8–11.
- [12] Rocha-Barbosa O, Moraes e Silva R. Analysis of the microstructure of Xenodontinae snake scales associated with different habitat occupation strategies. *Brazilian Journal of Biology*, 2009, **69**, 919–923.
- [13] Berthé R, Westhoff G, Bleckmann H, Gorb S. Surface structure and frictional properties of the skin of the Amazon tree boa *Corallus hortulanus* (Squamata, Boidae). *Journal of Comparative Physiology A*, 2009, **195**, 311–318.
- [14] Klein M-C G, Deuschle J K, Gorb S N. Material properties of the skin of the Kenyan sand boa *Gongylophis colubrinus* (Squamata, Boidae). *Journal of Comparative Physiology A*, 2010, **196**, 659–668.
- [15] Benz M J, Kovalev A E, Gorb S N. Anisotropic frictional properties in snakes. *SPIE Smart Structures and Materials+ Nondestructive Evaluation and Health Monitoring*, 2012, 83390X, <https://doi.org/10.1117/12.916972>.
- [16] Klein M-C G, Gorb S N. Epidermis architecture and material properties of the skin of four snake species. *Journal of the Royal Society Interface*, 2012, **9**, 3140–3155.
- [17] Marvi H, Hu D L. Friction enhancement in concertina locomotion of snakes. *Journal of the Royal Society Interface*, 2012, **9**, 3067.
- [18] Abdel-Aal H, El Mansori M. *Reptilian Skin as a Biomimetic Analogue for the Design of Deterministic Tribosurfaces*, Springer, 2011. (in Germany)
- [19] Abdel-Aal H A, El Mansori M. Tribological analysis of the ventral scale structure in a Python regius in relation to laser textured surfaces. *Surface Topography: Metrology and Properties*, 2013, **1**, 015001.
- [20] Baum M J, Heepe L, Fadeeva E, Gorb S N. Dry friction of microstructured polymer surfaces inspired by snake skin. *Beilstein Journal of Nanotechnology*, 2014, **5**, 1091–1103.
- [21] Baum M J, Heepe L, Gorb S N. Friction behavior of a microstructured polymer surface inspired by snake skin. *Beilstein Journal of Nanotechnology*, 2014, **5**, 83–97.
- [22] Greiner C, Schäfer M. Bio-inspired scale-like surface textures and their tribological properties. *Bioinspiration & Biomimetics*, 2015, **10**, 044001.

- [23] Mühlberger M, Rohn M, Danzberger J, Sonntag E, Rank A, Schumm L, Kirchner R, Forsich C, Gorb S, Einwögerer B. UV-NIL fabricated bio-inspired inlays for injection molding to influence the friction behavior of ceramic surfaces. *Microelectronic Engineering*, 2015, **141**, 140–144.
- [24] Cuervo P, López D, Cano J, Sánchez J, Rudas S, Estupiñán H, Toro A, Abdel-Aal H. Development of low friction snake-inspired deterministic textured surfaces. *Surface Topography: Metrology and Properties*, 2016, **4**, 024013.
- [25] Ren L. Progress in the bionic study on anti-adhesion and resistance reduction of terrain machines. *Science in China Series E: Technological Sciences*, 2009, **52**, 273–284.
- [26] Zheng L, Wu J, Zhang S, Sun S, Zhang Z, Liang S, Liu Z, Ren L. Bionic coupling of hardness gradient to surface texture for improved anti-wear properties. *Journal of Bionic Engineering*, 2016, **13**, 406–415.
- [27] Stidworthy J. *Snakes of the World*, Grosset & Dunlap Inc., USA, 1974.
- [28] Mehrtens J M. *Living Snakes of the World in Color*, Sterling Pub Co Inc, USA, 1987.
- [29] Wallach V, Williams K L, Boundy J. *Snakes of the world: A catalogue of living and extinct species*, CRC Press, USA, 2014.
- [30] Hisham A. On surface structure and friction regulation in reptilian limbless locomotion. *Journal of the Mechanical Behavior of Biomedical Materials*, 2013, **22**, 115–135.
- [31] Abdel-Aal H, El Mansori M, Mezghani S. Multi-scale investigation of surface topography of ball python (*Python regius*) shed skin in comparison to human skin. *Tribology Letters*, 2010, **37**, 517–527.
- [32] Abdel-Aal H A. Functional surfaces for tribological applications: inspiration and design. *Surface Topography: Metrology and Properties*, 2016, **4**, 043001.
- [33] Klein M-C G, Gorb S N. Scratch resistance of the ventral skin surface in four snake species (Squamata, Serpentes). *Zoology*, 2016, **119**, 81–96.
- [34] Voigt D, Schweikart A, Fery A, Gorb S. Leaf beetle attachment on wrinkles: Isotropic friction on anisotropic surfaces. *The Journal of Experimental Biology*, 2012, **215**, 1975.
- [35] Baum M J, Kovalev A E, Michels J, Gorb S N. Anisotropic friction of the ventral scales in the snake *Lampropeltis getula californicae*. *Tribology Letters*, 2014, **54**, 139–150.
- [36] Hutchings I M. Strain rate effects in microparticle impact. *Journal of Physics D: Applied Physics*, 1977, **10**, L179.
- [37] Carter G, Nobes M J, Arshak K I. The mechanism of ripple generation on sandblasted ductile solids. *Wear*, 1980, **65**, 151–174.
- [38] Ren L Q, Li J Q, Tong J, Chen B C. Bionic nonsmoothness and its applications. *Proceedings of the 6th Asia-Pacific Conference of ISTVS*, Shanghai, China, 2000, 351–358.
- [39] Tong J, Ma Y H, Ren L Q, Li J Q. Tribological characteristics of pangolin scales in dry sliding. *Journal of Materials Science Letters*, 2000, **19**, 569–572.
- [40] Sun J-R, Hong C, Qian C, Li J-Q, Chen B C, Ren L Q. Bionic study on the dung beetle *Copris ochus Motschulsky* for reduction of soil adhesion. *Acta Biophysica Sinica*, 2001, **17**, 785–793.
- [41] Ren L Q, Liang Y H. Generation mechanism of biological coupling. *Journal of Jilin University (Engineering and Technology Edition)*, 2011, **41**, 1348–1357. (in Chinese)
- [42] Ronen A, Etsion I, Kligerman Y. Friction-reducing surface-texturing in reciprocating automotive components. *Tribology Transactions*, 2001, **44**, 359–366.
- [43] Scaraggi M, Mezzapesa F P, Carbone G, Ancona A, Sorgente D, Lugarà P M. Minimize friction of lubricated laser-microtextured-surfaces by tuning microholes depth. *Tribology International*, 2014, **75**, 123–127.
- [44] Hu D L, Nirody J, Scott T, Shelley M J. The mechanics of slithering locomotion. *Proceedings of the National Academy of Sciences*, 2009, **106**, 10081–10085.
- [45] Alexander R M. *Principles of Animal Locomotion*, Princeton University Press, USA, 2003.